1 **Bromocarbons in the tropical coastal and open ocean atmosphere during the 2009**

2 **Prime Expedition Scientific Cruise (PESC-09)**

3 Mohd Shahrul Mohd Nadzir[a,b,c,*], Siew Moi Phang[c], Mhd Radzi Abas[a,c], Noorsaadah Abd. Rahman[a,c],

4 Azizan Abu Samah[b,c], , William T. Sturges[d], David E. Oram[d,g], Graham P. Mills[d], Emma C.

5 Leedham[d], J. A. Pyle[e,g], N. R. P. Harris[e], A. D. Robinson[e], M. J. Ashfold[e,**], M.I. Mead[e,***], Mohd

6 Talib Latif[h,i], Md. Firoz Khan[h], Negar Banan[h] and Abd Muhaimin Amiruddin[f]

7 [a] Environmental Research Group, Department of Chemistry, University Malaya, 50603 Kuala Lumpur

8 [b] National Antarctic Research Centre, IPS Building, University Malaya, 50603 Kuala Lumpur. Malaysia.

9 [c] Institute of Ocean & Earth Sciences, C308 IPS Building, University Malaya, 50603 Kuala Lumpur. Malaysia.

10 [d] Centre for Ocean and Atmospheric Sciences, School of Environmental Sciences, University of East Anglia,

11 Norwich, NR4 7TJ, UK

12 [e] Centre for Atmospheric Science, Department of Chemistry, University of Cambridge, Lensfield Road,

13 Cambridge, CB2 1EW.

14 [f] Department of Environmental Management, Faculty of Environmental Studies. Universiti Putra Malaysia.,

15 43400 Serdang, Selangor. Malaysia

16 [g] National Centre for Atmospheric Science, UK

17 [h] Research Centre for Tropical Climate Change System (IKLIM) , Faculty of Science and Technology,

18 Universiti Kebangsaan Malaysia.

19 [i] School of Environmental and Natural Resource Sciences, Faculty of Science and Technology, Universiti

20 Kebangsaan Malaysia.

21 [*] now at: School of Environmental and Natural Resource Sciences, Faculty of Science and Technology,

22 Universiti Kebangsaan Malaysia.

23 [**] now at: School of Biosciences, University of Nottingham Malaysia Campus, Jalan Broga, 43500 Semenyih,

24 Selangor Darul Ehsan, Malaysia.

25 [***] Now at: Institute of Ocean & Earth Sciences, C308 IPS Building, University Malaya, 50603 Kuala Lumpur.

26 Malaysia.

28   * Tel.: +60-389213861; fax: +60-389253357

29   E-mail address: shahrulnadzir@ukm.my

30

31   **Abstract**

32   Atmospheric concentrations of very short-lived species (VSLS) bromocarbons, including

33    $CHBr_3$, CH_2Br_2, $CHCl_2Br$, $CHClBr_2$, CH_2BrCl, were measured in the Strait of Malacca, the

34   South China and Sulu-Sulawesi Seas during a two month research cruise in June-July 2009.

35   The highest bromocarbon concentrations were found in the Strait of Malacca, with smaller

36   enhancements in coastal regions of Northern Borneo. $CHBr_3$ was the most abundant

37   bromocarbon, ranging from 5.2 pmol mol^{-1} in the Strait of Malacca to 0.94 pmol mol^{-1} over

38   the open ocean. Other bromocarbons showed lower concentrations, in the range of 0.8-1.3

39   pmol mol^{-1} for CH_2Br_2, 0.1-0.5 pmol mol^{-1} for$CHCl_2Br$ and 0.1-0.4 pmol mol^{-1} for $CHClBr_2$.

40   There was no significant correlation between bromocarbons and *in situ* chlorophyll-*a* but

41   positive correlations with both MODIS and SeaWiFS satellite's chlorophyll-*a*. Together the

42   short-lived bromocarbons contribute an average of 8.9 pmol mol^{-1} (range 5.2-21.4 pmol mol^{-}

43   ^{1}) to tropospheric bromine loading, which is similar to that found in previous studies from

44   global sampling networks (Montzka et al., 2011). Statistical tests showed strong Spearman

45   correlations amongst brominated compounds, suggesting a common source. Log-log plots of

46    $CHBr_3$/CH_2Br_2 versus $CHBr_2Cl$/CH_2Br_2 show that both chemical reactions and dilution into

47   the background atmosphere contribute to the composition of these halocarbons at each

48   sampling point. We have used the correlation to make a crude estimate of the regional

49   emissions of $CHBr_3$ and derive a value of 32 Gg yr^{-1} for the South East (SE) Asian region

50   (10°N-20°S, 90°E-150°E). Finally, we note that satellite-derived chlorophyll-*a* (chl-*a*)

51   products do not always agree well with *in situ* measurements, particularly in coastal regions

52   of high turbidity, meaning that satellite chl-*a* may not always be a good proxy for marine

53   productivity.

54

1 Introduction

56   In recent years there has been a growing interest in the role of short-lived halocarbons in

57   atmospheric chemistry, in particular their potential involvement in stratospheric ozone

58   depletion. The term very short-lived substances (VSLS) has been used to represent halogen-

59   containing compounds with lifetimes less than six months (WMO, 2007). Bromine-

60   containing VSLS and their atmospheric degradation products are believed to account for

61   around a quarter of total bromine entering the lower stratosphere (Dorf et al., 2006; Salawich

62   et al., 2006; Montzka et al., 2011) and contribute to the 'missing' bromine (6 pmol mol^{-1},

63   range 3-8 pmol mol^{-1}) required to the levels of inorganic bromine Br$_y$ and BrO measured in

64   the stratosphere (Montzka et al., 2011).

65   The main brominated VSLS identified to date include bromoform (CHBr$_3$),

66   dibromomethane (CH$_2$Br$_2$), dichlorobromomethane (CHCl$_2$Br), dibromochloromethane

67   (CHClBr$_2$) and bromochloromethane (CH$_2$BrCl). Biogenic emissions from the oceans have

68   been identified as one of the main natural sources, where organisms such as macroalgae

69   (seaweeds) and microalgae (phytoplankton) can release large quantities of halocarbon gases

70   to the atmosphere (Sturges et al., 1993; Moore et al., 1996; Laturnus and Adams, 1998).

71   Previous ship and coastal measurements have collected bromocarbon data for many different

72   global regions, summarised in Montzka et al. (2011). These studies show large temporal and

73   spatial variability in both seawater and atmospheric concentrations, emphasizing the

74   importance of localised emissions of these gases.

75   Because of their short atmospheric lifetimes, the region where VSLS are emitted into

76   the atmosphere is significant and their O_3 depletion potentials (ODPs) vary accordingly (Ko

77   et al., 2003). Tropical regions are believed to be the most important location for rapid

78   transport of air from the surface to the upper troposphere and lower stratosphere. In the

79   tropics, deep convection provides a major pathway for rapid transport of insoluble gases from

80   the lower to the upper troposphere. Importantly, such convective transport appears to be

81   particularly strong over the western Pacific (Gettelman et al., 2002; Fueglistaler et al., 2004).

82   Furthermore, the warm, shallow waters of the tropical warm pool make them potentially

83   important source regions for biologically-produced halocarbons. Therefore, this region has

84   the potential to supply a proportion of the 'missing' ~6 pmol mol^{-1} of bromine, thought to be

85   related to VSLS, to the stratosphere.

86   Yokouchi et al. (1997) were the first to report atmospheric bromocarbon

87   measurements in the Strait of Malacca and the South China Sea. During a cruise between

88   Japan and the Bay of Bengal they measured mean concentrations of 0.77 pmol mol^{-1} (max

89   1.42 pmol mol^{-1}) and 1.2 pmol mol^{-1} (max 7.1 pmol mol^{-1}) for CH_2Br_2 and $CHBr_3$,

90   respectively. The highest levels were seen in harbour regions of Singapore and Penang and

91   the authors suggested a link between high $CHBr_3$ concentrations and high chlorophyll-*a* (chl-

92   *a*) and the influence of algal sources. During a cruise in the South China Sea, Quack and

93   Suess (1999) observed mean ambient air concentrations for bromoform of 1.2 pmol mol^{-1}

94   (range 0.38-10.67 pmol mol^{-1}).

95   A second cruise reported in Yokouchi et al. (1997) was made in the western Pacific

96   (Japan-SE Australia) where atmospheric mixing ratios were observed in the range of 0.13-

97   2.9 pmol mol^{-1} for $CHBr_3$ and 0.14-1.58 pmol mol^{-1} for CH_2Br_2. More recently, Yokouchi et

98   al. (2005) reported a larger range of bromocarbon concentrations, with $CHBr_3$ ranging from

99   ~1 pmol mol^{-1} over the open ocean to ~40 pmol mol^{-1} in the vicinity of tropical islands in the

100 western Pacific region. Butler et al. (2007a) collected data from seven open ocean cruises

101 spanning a ten-year period, covering much of the world's oceans. Their tropical air mean

102 mixing ratios for $CHBr_3$ and CH_2Br_2 were 1 pmol mol^{-1} (0.4-2.1 pmol mol^{-1}) and 0.9 pmol

103 mol^{-1} (0.6-1.3 pmol mol^{-1}) respectively.

104   Despite these measurements collected over the last two decades, the seas and

105 coastlines of SE Asia are still vastly under-represented. This knowledge gap introduces

106 uncertainties in our understanding of the global distributions and fluxes of bromocarbons and

107 therefore in our ability to predict future changes in global fluxes and their impact on

108 stratospheric ozone and climate. Pyle et al. (2011) reported measurements of bromocarbons

109 from two land-based sites in Borneo covering 3 weeks in June and July 2008. The coastal

110 measurements were characterised by large variability, from a background of 2 to 5 pmol mol^{-}

111 ^{1} of $CHBr_3$ to occasional measurements of hundreds of pmol mol^{-1}. Measurements around the

112 island were generally much lower and less variable, more consistent with the background of

113 about 1 pmol mol^{-1}. The data were used to make an estimate of the regional emission strength

114 of $CHBr_3$ which, depending on assumptions, ranged between 21 and 50 Gg/yr in SE Asia

115 (10°N x 20°S, 90°E to 160°E). For the purpose of comparison we will also consider

116 tetrachloroethylene (C_2Cl_4), which has predominantly industrial uses as a metal degreasing

117 solvent, and dry cleaning and can be considered as a tracer of anthropogenic activity (Pyle et

118 al., 2011).

119   How representative these Borneo measurements are of the whole SE Asia region is an

120 important question and one that was addressed by the *Prime Expedition Scientific Cruise* in

121 2009 (PESC-09). Selected halocarbons, including the five bromomethanes detailed above,

122 were measured in air samples collected in three different areas: the Strait of Malacca (SM),

123   the South China Sea (SCS) and the Sulu-Sulawesi Seas (SSS). Samples were collected at

124   both coastal and open ocean locations, sometimes close to the sites mentioned in Pyle et al.

125   (2011). The cruise and measurement details are presented in section 2. Results are presented

126   and discussed in section 3.

127

128   **2 Measurements**

129   **2.1 Cruise details**

130   The PESC-09 cruise was conducted by the Malaysian Royal Navy and Malaysian Ministry of

131   Science and Technology Innovation (MOSTI) and involved local government, private

132   research agencies and public universities in Malaysia. The vessel used was the Kapal Diraja

133   (Royal Ship) Perantau, which is designed and equipped for hydrographic surveying and for

134   conducting meteorological and oceanographic observations. The cruise started from Port

135   Klang (2°57' N101°20' E) in the Strait of Malacca, on 18th June and ended at, Kota Kinabalu

136   (6$^{°}$11'N116$^{°}$10$^{'}$E) on 31st July. These paths were separated into four different legs: leg one

137   (Port Klang-Labuan); leg two (Labuan-Layang-layang Island-Kota Kinabalu); leg three (Kota

138   Kinabalu-Tawau) and leg four (Tawau- Kota Kinabalu). Figure 1 shows the ship's route

139   together with the location of the 27 air sampling stations.

140   During the seven week cruise, several different oceanic regions were covered, including

141   SM, SCS and SSS seas, and coastal regions of western and northern Borneo. Mangrove

142   forest, sea grass beds and coral reefs dominate much of the coastline and, in northern Borneo

143   in particular, there are areas of cultivated macroalgal beds along the coastline at sites such as

144   Semporna, Kunak and Lahad Datu. The sampling locations were chosen to represent a variety

145   of coastal and open ocean sites.

2.2 Sampling and measurements

Air was sampled through a 1/4″OD PFA tube located on the upper deck with the inlet ~10m above the ocean surface and adjusted at each sampling time to face the prevailing wind. Air was pumped into a pre-evacuated 3-litre canister (Restek SilcoCan™) using a compact, battery-operated diaphragm pump (Rasmussen) until the canisters were approximately two atmospheres above ambient pressure (approximately five minutes of sampling). Canisters were filled and vented at least three times, before a final fill which was kept for analysis. A total of 27 air samples were collected during the cruise, and these were shipped to the University of East Anglia (UK), for halocarbon analysis by GC-MS (gas chromatography - mass spectroscopy).

The samples were processed within four months of collection using a commercial thermal desorption system (Markes UNITY^{TM}/Air Server). The analytical technique was similar to that described by Worton et al. (2008). Air samples (1000 ml) were dried with a Nafion™ counter-flow dryer prior to collection and pre-concentration on a 2-bed adsorbent trap at -15°C. The desorbed analytes were separated on a capillary column (Restek 100 m x 0.32 mm RTX 102) using a temperature programme of 30$^{°}$C (2 min), 8$^{°}$C/min to 150 $^{°}$C (16 min), 20$^{°}$C/min to 220$^{°}$C (5min). The mass spectrometer was operated in negative ion, chemical ionisation (NICI) mode using methane (≥99.99%) as the reagent gas. The quadrupole detector was run in single ion mode, monitoring m/z 35/37 for chlorinated, m/z 79/81 for brominated and m/z 127 for iodinated compounds. Samples were normally analysed twice and referenced to a working standard. The working standard was an aluminium cylinder containing dried ambient air at high pressure. The mole fractions of halocarbons in the working standard were determined by repeat comparison to calibrated gas standards supplied by NOAA-ESRL in electropolished stainless steel canisters (Essex Industries).

170   These comparisons are performed periodically and allow an assessment of any potential

171   changes in the absolute mole fractions of halocarbons in our working standard over time.

172   From comparisons with three separate NOAA standards: SX-3546 (comparison performed in

173   2008); SX-3570 (2010); and SX-3568 (2012) we believe the concentration of $CHBr_3$ in the

174   working standard has declined by approximately 40% over the period October 2008-

175   September 2012, whilst that of CH_2Br_2 has remained essentially unchanged (1.23 ± 0.07

176   pmol mol^{-1}, or 5.6%, 1σ). NOAA calibration data for the three mixed bromochloromethanes

177   were only available for the 2010 and 2012 comparisons, but our analysis shows that the

178   concentrations of CH_2ClBr and $CHClBr_2$ in the working standard have remained

179   approximately constant (0.28 ± 0.004 pmol mol^{-1}, or 1.5%; and 1.18 ± 0.04 pmol mol^{-1}, 3.2%

180   respectively) whilst that of $CHCl_2Br$ may have increased by around 15% (1.56 ± 0.17 pmol

181   mol^{-1}, or 10.6%). The calibration factors applied to the PESC-09 data have been time-

182   corrected as appropriate. This drift analysis makes the underlying assumption that the five

183   bromocarbons are reliably stored in the Essex stainless steel cylinders.

184   The mole fractions reported here are on the latest NOAA scales for CH_2Br_2 (2004)

185   and $CHBr_3$ (2003), and on a preliminary NOAA scale for CH_2BrCl, $CHBrCl_2$ and $CHBr_2Cl$

186   (Brad Hall, personal communication). The uncertainty in the absolute mole fractions in the

187   working standard, based on combined uncertainties associated with the standard comparisons

188   and NOAA's stated uncertainties was ± 6.5% for CH_2Br_2, ± 7.1% for $CHBr_3$, ± 7.5% for

189   CH_2ClBr, ± 5.9% for $CHCl_2Br$ and ± 6.8% for $CHClBr_2$. Mean analytical precision of the

190   actual PESC-09 samples was <3% for CH_2Br_2 and $CHBr_3$, <5% for $CHBrCl_2$ and $CHBr_2Cl$,

191   and ~15% for CH_2BrCl, due to its low abundance and low response in NICI).

192   Chl-a in the surface seawater was measured using the Kapal Diraja (KD) Perantau's

193   in-situ fluorometer attached to Sea-Bird SBE-911plus CTD (conductivity, temperature,

194 depth) system at all 27 sampling locations. The CTD equipment was operated together with a

195 package consisting of a 24-place, 10-liter rosette frame, a 24-place water sampler (SBE32)

196 and 24, 10-liter Niskin bottles sampler. This package was deployed at all stations. Several

197 fluorometers, turbidity sensors and pH measurements were attached to the CTD. The CTD

198 instrument was run and calibrated automatically at each station before sampling. The chl-*a*

199 concentration was measured from 1 m to 20 m depth with 5 m intervals. Readings were taken

200 at the sea surface approximately 1 m depth and have been compared with satellite-derived

201 chl-*a* data from SeaWIFS (Sea-Viewing Wide Field-of-view Sensor) and MODIS (Moderate

202 Resolution Imaging Spectroradiometer). Chl-*a* derived from ocean colour measurements

203 made during overpasses of the SeaWIFS and Aqua-MODIS satellite sensors were used to

204 determine apparent chl-*a* values in the nearest 9x9 km grid square to each sampling point.

205 The corresponding monthly average chl-*a* values (i.e. those for either June or July) were

206 used, obtained from the NASA Goddard 'Giovanni' on-line database

207 (http://oceancolor.gsfc.nasa.gov/SeaWiFS/). Shorter averaging periods are available (e.g. 8-

208 day) but were found to be insufficient for full coverage of the cruise track given the width of

209 the viewing swath, the level of missing data on several overpasses, and differences between

210 satellite sensors in ocean colour-derived chl-*a*. There is a substantial difference in both the

211 temporal and spatial scales between the monthly-averaged and 9x9 km grid-box averaged

212 satellite measurements and the near-instantaneous *in situ* 'spot' measurements. As an

213 indication of the level of uncertainty (at least that related to spatial scales) the standard

214 deviation of satellite-determined chl-*a* was calculated for the eight to ten grid boxes

215 surrounding and including the target grid box, depending on the values at each location

216 (negative values were not considered).

217

3. Results and Discussion

In the following sections we will, first, present an overview of the halocarbon data collected during PESC-09 (section 3.1). We then discuss possible causes of any observed variability, focussing on an analysis of air parcel trajectories and *in situ* measurements of chl-*a*, which are a possible proxy for biological activity (section 3.2). In section 3.3 we explore correlations between the measured species and provide a rough estimate of regional bromoform emissions. Finally (section 3.4) we use the data to investigate the potential contribution of VSLS to stratospheric bromine loading.

3.1 Halocarbon measurements

Mean and standard deviation of the measured halocarbon concentration at each site are given in Table 1 along with some comparison with data from the literature. Figure 2 shows the concentrations of brominated compounds ($CHBr_3$, CH_2Br_2, $CHBr_2Cl$, $CHBrCl_2$ and CH_2BrCl) at each of the cruise sampling sites, whose locations are marked on Figure 1. The most abundant bromine compound was $CHBr_3$, with mean concentrations from around 1pmol mol^{-1} to more than 5 pmol mol^{-1} (mean = 1.85 pmol mol^{-1}, max = 5.2 pmol mol^{-1}). Most measurements are between 1 and 2 pmol mol^{-1}. The mean mixing ratio of CH_2Br_2 was 1.23 pmol mol^{-1} (max = 2.21), with the minor species $CHBr_2Cl$, $CHBrCl_2$ and CH_2BrCl having mixing ratios in the mean 0.1 to 0.9 pmol mol^{-1}. For the anthropogenic tracer C_2Cl_4, mixing ratios varied only between 0.9 and 1.0 pmol mol^{-1}. The PESC-09 measurements are generally within the range of previous measurements in tropical regions.

241 **3.2 Regional analysis**

242 **3.2.1 Strait of Malacca** (Stations 1-4).

243 PESC-09 took place during the South West Monsoon (SWM) when sea surface temperatures

244 are slightly warmer (28-32°C, May/June) than in the North West Monsoon (NWM) (25-29°C,

245 December/January). Tan et al. (2006) report that chl-a in the Strait of Malacca shows

246 seasonal variability with concentrations increased by as much as a factor of two (0.57 mgm^{-3}

247 in August and 1.38 mgm^{-3} in January 1992-2002 monthly average) during NEM compared to

248 SWM.

249   The highest concentrations of CHBr$_3$ were observed at the beginning of the cruise in the

250 Strait of Malacca (SM). The mean concentration in samples 2-4 was 4.4 pmol mol^{-1}, which is

251 similar to the levels in the same region reported by Yokouchi (1997). The enhanced levels

252 may be related to the high population of macro and micro algae such as phytoplankton and

253 seaweeds at coastal areas, especially in the region of 1-2°N, 102-103°W. Previous studies on

254 chl-a in the SM were influenced by nutrient input from rivers of Sumatra (Tan et al., 2006).

255 CH$_2$Br$_2$, CHCl$_2$Br, CHClBr$_2$ and CHCl$_3$ were also enhanced in samples 2-4, which is

256 indicative of similar sources.

257

258 **3.2.2 South China Sea (Stations 5 to 14)**

259 Measurements in the SCS show fairly uniform and relatively low mixing ratios for all

260 brominated compounds. For example, the mean values for CHBr$_3$, CH$_2$Br$_2$ and CHBr$_2$Cl were

261 1.46, 1.12 and 0.35 pmol mol^{-1} respectively, with no significantly enhanced values. The

262 prevailing wind direction for most samples collected along this section of the cruise was

263 westerly, so the influence of any local coastal emissions would likely be low.

3.2.3 Sulawesi and Sulu Seas (Stations 15-27)

Slightly higher concentrations of bromocarbons were observed during the cruise through the SSS, especially at Station 22 and 24 where $CHBr_3$ concentrations were 2.37 and 2.60 pmol mol^{-1} respectively. During this period the ship passed near to coastal sites at Semporna (station 22), Kunak (19, 20, 21, 27) and Tawau (24, 26). The coastal areas near Semporna and Kunak have significant seaweed biomass, with cultivated *Kappaphycus* and *Eucheuma* at Semporna and *Sargassum* and other brown algae at Kunak. Samples 17 and 21 had slightly elevated levels of C_2Cl_4, suggesting a possible influence from local anthropogenic sources.

Pyle et al. (2011) measured $CHBr_3$ concentrations at Kunak ranging from a typical background of 2-5 pmol mol-1, but high concentration up to 60 pmol mol^{-1} (the latter were attributed to measurement very close to local emissions). During their short measurement period in July 2008 the air flow was predominantly from the south east, with back-trajectories showing air travelling from northern Australia, over the Timor and East Java Seas and up the eastern coast of Borneo. The authors speculated that these are areas of high biological activity, with both the warm ocean and extensive coastline providing significant sources of halocarbons. Despite similar air mass back-trajectories and sampling in similar locations, we did not measure the very high levels of $CHBr_3$ reported by Pyle et al. (2011). For example, at station 27, back-trajectories did not indicate that air flow had passed any seaweed or high nutrient area.

3.3 Drivers of variability

288   The data collected during PESC-09 show relatively small variability, consistent with the ship

289   data reported by Yokouchi et al. (1997) over the western Pacific and South East Asia (see

290   Table 1). For example, Yokouchi observed mixing ratios of $CHBr_3$ of 0.32 to 7.1 pmol mol^{-1}

291   which is similar to our study, with a range of 1.85-5.25 pmol mol^{-1} for $CHBr_3$. This contrasts

292   with the study of Yokouchi et al. (2005) over western Pacific and Java Island, who observed

293   high mixing ratios with a range of 16.3 to 31.4 pmol mol^{-1} at Christmas Island, and 4.2 to

294   43.6 pmol mol^{-1} at San Cristobal Island. Pyle et al. (2011) also observed high mixing ratios of

295    $CHBr_3$ in Malaysian Borneo (near to station 21 and 27 in this study), with a range of 2 to 60

296   pmol mol^{-1}. It seems likely that these latter studies both included data collected close to

297   emission sources.

298   Atmospheric variability is driven by various factors including wind direction,

299   atmospheric lifetime, proximity to local sources and temporal variation of flux rates. Changes

300   in VSLS emissions could arise from a number of complex factors. Emissions of VSLS are

301   predominantly biogenic, with the ocean being the most important source (Baker et al., 2000;

302   Quack et al., 2004). Proximity to local seaweed beds (including seaweed farms) is likely to be

303   an important influence in coastal regions. In the case of microalgae, their abundance and

304   distribution in seawater are affected by nutrient supplies and sea surface temperatures, while

305   sea-air fluxes of VSLS are determined by meteorological parameters including wind speed.

306   Chl-*a* can be used as a simple proxy for biological activity, possibly producing halocarbons,

307   which may be emitted into the atmosphere, depending on concentrations and wind speed.

308

309

310

3.3.1 Meteorological variability

A major factor controlling the variability of the halocarbon concentrations during the cruise is the wind direction. Figure 3 shows selected 10-day air mass back trajectories for seven of the cruise sampling locations calculated from the NOAA HYSPLIT model (R. R. Draxler and G. D. Rolph, HYSPLIT- Hybrid Single-Particle Lagrangian Integrated Trajectory), available at http://www.arl.noaa.gov/ready.html). In all cases the large-scale structure is consistent. Air masses arriving at the sampling locations originated to the south east and have likely been influenced by emissions from shallow, warm seas, including the South Java Sea. There is therefore likely to be little variability associated with transport from different large-scale emission regions, although local emissions close to the sampling locations could still be important in driving local variability. For example, the trajectories arriving at site 22, near Sipadan Island, or at station 19, near Kunak, are very likely to have been influenced by the seaweed beds in that area. A similar conclusion was reached by Pyle et al. (2011) based on their coastal Kunak measurements in June 2008, made one year earlier than the PESC-09 cruise and the origins of the measured air masses were very similar in both years.

3.3.2 Biological activity

Chl-*a* was also measured at 60 sites including 27 sites where halocarbons are measured during the cruise, both *in situ* from the ship and remotely from satellite sensors. We compare the chl-*a* measurements with the halocarbon data to explore possible biological drivers of variability. Figure 1 plots the monthly average chl-*a* across the region from SeaWiFS for June 2009 overlaid with the sampling stations. High chl-*a* levels are commonly observed along the coastlines, seemingly indicating high phytoplankton abundance. Indeed high satellite-derived chl-*a* values were evident in the Strait of Malacca, where the highest $CHBr_3$

335   was measured. However, a plot of ocean colour-derived chl-*a* from the two satellite sensors

336   versus *in situ* chl-*a* (Figure 4) shows significant disagreement between the remotely-sensed

337   and *in situ* measurements. The standard deviations from the target grid box and those

338   surrounding it are in the range of 1.1 to 32.4 mgm^{-3} for MODIS and 0.1 to 18.2 mgm^{-3} for

339   SeaWiFS.

340   In Figure 4, the filled symbols denote samples in which the turbidity was >0.5 FTU

341   (Formazin turbidity unit), whereas open symbols denote low turbidity (<0.5 FTU). It is

342   apparent that the low turbidity samples display a relatively compact relationship between

343   remotely-sensed and *in situ* chl-*a* and with absolute values that are in good quantitative

344   agreement. Indeed a linear regression on the lower turbidity samples yields a gradient of 1.0

345   (standard error of 0.1) and an r^2 value of 0.88. The points that do not follow the positive

346   linear regression line are characterised by satellite chl-a concentrations greater than 1 mg m^{-3},

347   and turbidities greater than 0.5 FTU, implying that the satellite sensors over-estimate chl-*a*

348   under such conditions. Indeed the *in situ* measurements showed that ship-board

349   measurements of chl-*a* are lower than those made in the open ocean. We reiterate (refer back

350   to Section 2.2) that there are difficulties in comparing coarse satellite data with *in situ*

351   measurements, but believe this type of comparison still provides valuable information from a

352   data-sparse region.

353   Plots of bromocarbon air concentration versus satellite chl-*a* concentration (Figure 5)

354   show a positive correlation, with the highest mixing ratios of $CHBr_3$ and CH_2Br_2 associated

355   with above average chl-*a* values (> 5 mgm^{-3}) for MODIS and SeaWiFS satellites. Both

356   satellite chl-*a* products show R values > 0.6 against $CHBr_3$ and CH_2Br_2 (also $CHBr_2Cl$ for

357   MODIS) but other species show little correlation for both satellite chl-*a* products. *In situ* chl-

358   *a* concentrations show negative correlation for all bromocarbons species with r=-0.26

359   (p>0.01) and r=-0.21 (p>0.01) for $CHBr_3$ and CH_2Br_2, respectively (see figure 5). The exact

360   reason for the weak correlation of the bromocarbons and the *in situ* chl-*a* data is unclear.

361   The above finding is not necessarily surprising even if phytoplankton are a source of

362   such gases, since a connection between bromocarbons measured in the marine atmospheric

363   boundary layer and sub-surface biology may be dependent on other factors including wind

364   speed. Furthermore, the observed halocarbon concentrations might originate over a wide

365   geographic area and are not necessarily driven solely by localised emissions. In this context,

366   satellite-derived chl-*a*, also providing information from a wider area, may potentially be more

367   relevant than *in situ* measurements. Although turbidity measurements in the Strait of Malacca

368   (average of 3.3 FTU) were significantly higher than those in the South China Sea (average of

369   0.3 FTU; Table 1), coinciding with high $CHBr_3$, the turbidity was almost as high close to land

370   near Semporna (average of 2.1 FTU for Stations 24-27), but with little evidence of

371   substantially enhanced halocarbons in the latter region due to the lower marine productivity

372   especially at the coastal and open ocean region of SCS (Figure 1). We conclude that

373   halocarbon concentrations are generally somewhat higher close to land and also higher in the

374   Strait of Malacca, thus a connection to the coastal zone is suspected, but there is little

375   evidence to connect this directly to open ocean microorganisms.

376

377   **3.4 Emission ratios**

378   Significant correlations between brominated halocarbons have been observed in coastal air

379   measurements suggesting that these gases have come from the same sources (Yokouchi et al.,

380   2005; O'Brien et al., 2009; Carpenter et al., 2009). Several studies have exploited these

381   correlations to explore the possible source strengths of the individual species. Carpenter et al.

382 (2003), Yokouchi et al. (2005) and O'Brien et al. (2009) all show that a log-log plot of

383 $CH_2Br_2/CHBr_3$ versus $CHBr_3$ often shows a straight line with the ratio $CH_2Br_2/CHBr_3$

384 increasing with decreasing $CHBr_3$. Atmospheric ratios of $CH_2Br_2/CHBr_3$ are often interpreted

385 in the light of their differing atmospheric lifetimes, which are about 26 days for $CHBr_3$ and

386 120 days for CH_2Br_2 (Montzka et al., 2011). The relationship between $CHBr_3$ and other

387 somewhat longer-lived brominated halocarbons such as $CHBr_2Cl$ also showed similar

388 patterns, for example $CHBr_2Cl/CHBr_3$ would be higher at lower concentration of $CHBr_3$.

389 Since $CHBr_3$ has the shorter lifetime of the two species, an increase in the ratio would be

390 consistent with more aged air masses, in which $CHBr_3$ has been removed at a faster rate.

391 Yokouchi et al. (2005) used the minimum ratio of $CH_2Br_2/CHBr_3$ to define the ratio of the

392 emission sources by assuming that the emissions came from the common sources and are

393 constant on a regional scale. If the global emission of CH_2Br_2 is known, then that of $CHBr_3$

394 can be inferred. However the emission ratio for $CH_2Br_2/CHBr_3$ in the open ocean is different

395 (i.e. higher) to that in coastal areas and so the assumption of a single characteristic seawater

396 ratio is invalid, along with the extrapolation of source strength.

397 Figure 6 shows the relationships between CH_2Br_2 and $CHBr_3$ and between $CHBr_2Cl$

398 and $CHBr_3$ for each data set. Correlations are strong between CH_2Br_2 and $CHBr_3$ (correlation

399 coefficient, r = 0.9), $CHBr_3$ and $CHBr_2Cl$ (r = 0.7) and $CHBr_3$ and $CHBrCl_2$ (correlation

400 coefficient r = 0.5) (not shown in the figure). These variations in correlation are consistent

401 with the relationships observed in recent studies of the strength of emission of these different

402 compounds from a range of Malaysian seaweeds (Leedham et al., 2013; Seh-Lin Keng et al.,

403 2013). Figures 7a and 7b show the concentration ratios of $CH_2Br_2/CHBr_3$ and

404 $CHBr_2Cl/CHBr_3$ plotted against $CHBr_3$ on a log-log scale, with both ratios increasing linearly

405   as $CHBr_3$ decreases; $CHBr_3$, with its shorter lifetime, is a possible measure of time since co-

406   emission. These figures are consistent with those reported by Yokouchi et al. (2005).

407   Yokouchi et al. (2005), following McKeen and Liu (1993), used plots of pairs of

408   ratios, e.g. $CHBr_3/CH_2Br_2$ versus $CHBr_2Cl/CH_2Br_2$, where CH_2Br_2 has the longest lifetime, to

409   explore the possible emission strengths of the individual species. Making a number of

410   assumptions, in such a plot the location of individual points in ratio space is determined by

411   the emission ratio at an (assumed) common regional source and by the ratio of the rates of

412   chemical removal and mixing into the 'background' atmosphere. Assuming that the emission

413   source strength of one species is known, that of the others can be obtained using the ratio

414   determined from the plot. Using this method, O'Brien et al. (2009) estimated a global

415   emission of bromoform of 823-1404 Gg/yr (values depend *inter alia* on the assumed CH_2Br_2

416   emissions) using data collected at Cape Verde in June 2006. This emission is much higher

417   than estimates in Ko et al. (2003), or in Warwick et al. (2006). However, Pyle et al. (2011)

418   suggest that it is not reasonable to derive global emission estimates from regional data for a

419   short-lived species such as bromoform. They showed that data from Borneo could instead

420   only be used to constrain regional emissions.

421   Using data from the cruise, $CHBr_3/CH_2Br_2$ is plotted against $CHBr_2Cl/CH_2Br_2$ in

422   Figure 7b. The left side of the triangle is the 'dilution line' (the 1:1 slope for mixing into a

423   zero background) and the 'chemical decay line', defined by the ratio of lifetimes of individual

424   species due to photochemistry, is the right hand line. The intersection of these 2 lines, a point

425   typically chosen to allow the lines to encompass the majority of the data, defines the emission

426   ratios. Nearly all the data falls into a triangle whose vertex for $CHBr_3/CH_2Br_2$ takes a value

427   of 5 (point D on the figure). This is about half the value reported by Yokouchi et al. (2005)

428   and O'Brien et al. (2009) but similar to the result obtained by Brinckmann et al. (2012) based

429   on data collected in a recent western Pacific cruise. If we assume that this emission ratio of 5

430   is appropriate to the SE Asian Region, (10°N to 20°S, 90°E to 160°E, as used by Pyle et al.

431   (2011)) and recalling that the air mass histories in the two periods of these two studies are

432   quite similar, then we could derive an emission estimate for $CHBr_3$ from the regional CH_2Br_2

433   emission. That value is not observationally constrained; instead we use the SEA regional

434   CH_2Br_2 emission from an updated version of the Warwick et al. (2006) inventory (as used by

435   Yang et al., 2014). As before, spatially uniform ocean emissions of CH_2Br_2 are assumed in

436   the tropics, but emissions are halved so that the global total of 57 Gg CH_2Br_2/yr is more

437   consistent with the recent studies of Liang et al. (2010) and Ordonez et al. (2012). In that

438   case, with a SEA CH_2Br_2 emission of 6.4 Gg/yr, we obtain a regional emission, based on

439   point D from figure 7b, of about 32 Gg/yr of $CHBr_3$. This value is within the range obtained

440   by Pyle et al (2011), who estimated emissions of $CHBr_3$, for the same area, to be between 21

441   and 50 Gg/yr. It is also consistent with the recent work of Ashfold et al. (2014), who

442   estimated a total tropical $CHBr_3$ emission of 225 Gg/yr; simply scaling this tropical number

443   down (using the ratio of areas) to the SEA region considered here implies a $CHBr_3$ emission

444   of 33 Gg/yr. Our estimates, and those of Pyle et al. (2011) and Ashfold et al. (2014), are all

445   much less than the regional value in Warwick et al. (2006). To be more confident about our

446   emission value would require, amongst other things, improved estimates of the CH_2Br_2

447   emission. However, the consistency of the calculations does suggest that useful constraints on

448   regional estimates can be obtained based on McKeen and Liu (1993) plots.

449

450   **3.5 Total bromine**

451   The cruise data can be used to give an upper limit on the amount of bromine which could

452   potentially reach the stratosphere, i.e. by summing the measured bromine mixing ratios and

453   weighting by the number of bromine atoms. The mean VSLS-derived bromine ([Br]$_{VSLS}$) in

454   the 27 samples was 8.9 ± 3.7 pmol mol^{-1}. There is some regional variability as discussed

455   earlier, with SM having the highest [Br]$_{VSLS}$ (mean = 17.8 pmol mol^{-1}) compared to other

456   sampled areas. Of this 8.9 pmol mol^{-1}, CHBr$_3$ contributes ~65% and CH$_2$Br$_2$ 25%. This is

457   similar to results compiled by Montzka et al. (2011) for which an average total bromine from

458   the same gases in the tropical marine boundary layer (mostly from open ocean

459   measurements) is given as 8.4 pmol mol^{-1} with a range of 3.6–13.3 pmol mol^{-1}. With the

460   exception of the Strait of Malacca, there does not appear to be a large regional enhancement

461   of [Br]$_{VSLS}$ in our data, despite the cruise having taken place mostly within 50 km of the

462   coast. The data do not suggest that this part of SE Asia is a 'hot spot' for emissions.

463   The [Br]$_{VSLS}$ measured during the PESC-09 cruise are likely to account for some of

464   the 'missing' bromine entering the stratosphere, assuming conservative transport of the

465   constituent bromine either in the form of the source gas itself, or as brominated product

466   gases.

467

468   **4. Conclusions**

469   We report *in situ* halocarbon and ancillary data obtained during a research cruise of

470   the Perantau in June and July 2009. The cruise covered the Strait of Malacca, the South China

471   Sea and the Sulu and Sulawesi Seas. These are warm, shallow ocean areas and contain

472   conditions likely to support high halocarbon production and emission to the atmosphere. The

473   region is also important as a location of the strongest convection, therefore it thus represents

474   potentially an important source region for the transport of marine boundary layer

475   concentrations of VSLS to the upper troposphere and stratosphere.

476   Data were collected at 27 sites during the cruise. High bromoform concentrations (4-5

477   pmol mol^{-1}) were measured in the nutrient rich Strait of Malacca. Otherwise concentrations

478   were generally between 1 and 2 pmol mol^{-1}. This is consistent with an earlier cruise reported

479   by Yokouchi et al. (1997). Slightly higher concentrations were measured close to seaweed

480   farms in Semporna but nowhere on the cruise did we find very high concentrations similar to

481   those reported by Pyle et al. (2011) at a coastal site at Kunak, believed to be close to emission

482   sources. Further, there is no evidence from the cruise data that local emission sources in this

483   region lead to widespread, elevated concentrations ('hotspots') which might make a

484   contribution to stratospheric input out of proportion to the area of the region.

485   Our measurements of other compounds, including the less often reported mixed

486   chloro-bromocarbons, are also reasonably consistent with the few other studies in the region

487   (e.g. Quack and Suess, 1999; Yokouchi et al., 1997, see table 1). Our typical concentrations

488   of CH_2Br_2 ~1 pmol mol^{-1}, $CHBr_2Cl$ ~0.2-0.4 pmol mol^{-1}, $CHBrCl_2$ ~0.2-0.3 pmol mol^{-1} and

489   CH_2BrCl ~0.1-0.2 pmol mol^{-1} lead to a $[Br]_{VSLS}$ of 8.9 pmol mol^{-1}. This is close to values

490   obtained by Sala et al., (2014) from measurements collected in the planetary boundary layer

491   of the same region during the SHIVA campaign (7.8 and 9.1 pmol mol^{-1} using two separate

492   instruments). The similarity suggests boundary layer VSLS mixing ratios in this important

493   region are beginning to be better characterised.

494   The bromocarbons were well correlated, suggesting common sources. Previously,

495   such relationships have been used to obtain global emission estimates. For a short-lived gas

496   like bromoform, with an atmospheric lifetime of ~26 days, we do not think this approach is

497   suitable; the footprint sampled by the cruise is regional at most. Instead, we used an approach

498   as applied by Yokouchi et al. (2005) to provide a very rough estimate of the regional (S.E.

499   Asia) emission ratio of bromoform to dibromomethane of about 5. Using the

500   dibromomethane emissions from Liang et al. (2010) leads to bromoform emissions of 32 Gg

501   yr^{-1} for S.E. Asia (10°N to 20°S, 90°E to 160°E), which is in reasonable agreement with the

502   recent estimates from Pyle et al. (2011) and Ashfold et al. (2014). Much more data, not least

503   on CH_2Br_2 emissions, would be required to confirm this estimate, but the use of species

504   correlations for regional emission estimates looks to be a promising approach.

505   Chl-*a* was also measured on the cruise. There was little obvious correlation between

506   this and the measured atmospheric halocarbon concentrations. Satellite measurements of chl-

507   *a* suggested high values in the Strait of Malacca, coinciding with high turbidity and high

508   halocarbon concentrations. However, it seems likely that the satellite data were affected by

509   the high turbidity in these waters, and the underwater *in situ* chl-*a* measurements were similar

510   to those observed in the open sea. It seems likely that the higher halocarbon concentrations in

511   the Strait maybe result from local influence of the nearby coastal areas and land masses.

512   The seas around South East Asia are important for a number of atmospheric

513   processes, including both convection and the emission of brominated halocarbons.

514   Measurements of brominated halocarbons in this region are sparse, and despite the new

515   measurements reported here, the region remains data poor.

516

517

518

519

520

521

Acknowledgements

References

Ashfold, M. J, Harris, N. R. P., Robinson, A. D., Warwick, N. J., and Pyle, J. A., Estimates of tropical bromoform emissions using an inversion method. Atmos. Chem. Phys., 14, 979-994, 2014.

Baker, A. R., S. M. Turner, W. J. Broadgate, A. Thompson, G. B. McFiggans, O. Vesperini, P. D. Nightingale, P. S. Liss, and T. D. Jickells , Distribution and sea-air fluxes of biogenic trace gases in the eastern Atlantic Ocean, Global Biogeochem. Cycles, 14(3), 871–886, 2000.

Brinckmann, S., Engel, A., Bönisch, H., Quack, B., Atlas, E., Short-lived brominated hydrocarbons – observations in the source regions and the tropical tropopause layer, Atmos. Chem. Phys., 12, 1213-1228, 2012

Butler, H. J., King, B. D., Lobert, M. J., Montzka, A. S., Yvon-Lewis, A. S., Hall, D. B., Warwick, Mondeel, J. D., Aydin, M., Elkins, W. J., Oceanic distribution and emissions of short-lived halocarbons, Global Biogeochem. Cycles, 21, 1023, doi:10.1029/2006GB002732, 2007a.

Carpenter, L. J., Liss, P. S., and Penkett, S. A.: Marine organohalogens in the atmosphere over the Atlantic and Southern Oceans, J. Geophys. Res., 108(D9), 4256, doi:10.1029/2002JD002769, 2003.

567   Carpenter, L. J., Jones, C. E., Dunk, R. M., Hornsby, K. E., and Woeltjen, J.: Air-sea fluxes

568   of biogenic bromine from the tropical and North Atlantic Ocean, Atmos. Chem. Phys., 9,

569   1805–1816, 2009.

570

571   Dorf, M., J. H. Butler, A. Butz, C. Camy-Peyret, M. P. Chipperfield, L. Kritten, S. A.

572   Montzka, B. Simmes, F. Weidner, and K. Pfeilsticker, Observations of long-term trend in

573   stratospheric bromine reveal slowdown in growth, Geophys. Res, Lett., 33, L24803,

574   doi:10.1029/2006GL027714, 2006.

575

576   Fueglistaler, S., Wernli, H. and Peter, T., Tropical troposphere to stratosphere transport

577   Kinferred from trajectory calculations, J. Geophys. Res., 109, D03108,

578   doi:10.1029/2003JD004069, 2004.

579

580   Fueglistaler, S., Dessler, A. E., Dunkerton, T. J., Folkins, I., Fu, Q., and Mote, P. W.:

581   Tropical Tropopause Layer, Rev. Geophys., 47, RG1004, 443, 2009.

582

583   Gettelman, A., Salby, M.L. and Sassi, F., The distribution and influence of convection on the

584   tropical tropopause region, J. Geophys. Res., 107, 4080, doi:10.1029/2001JD001048, 2002.

585

586   Ko, M. K. W., Poulet, G., Blake, D. R., Boucher, O., Burkholder, J. H., Chin, M., Cox, R. A.,

587   George, C., Graf, H.-F., Holton, J. R., Jacob, D. J., Law, K. S., Lawrence, M. G., Midgley, P.

588   M.,Seakins, P. W., Shallcross, D. E., Strahan, S. E., Wuebbles, D. J., Yokouchi, Y., and

589   contributors: Very Short-Lived Halogen and Sulfur Substances, Scientific Assessment of

590   Ozone Depletion: 2002, World Meteorological Organization Global Ozone Research and

591   Monitoring Project – Report No. 47, Geneva, Switzerland, 2.1–2.57, 2003.

592

593   Laturnus, F and Adams, F. C.,: Methyl halides from Antarctic macroalgae. Geophys. Res.

594   Lett, 25, 773-776, 1998.

595

596   Leedham, E. C., Hughes, C., Keng, F. S. L., Phang, S.-M., Malin, G., and Sturges, W. T.:

597   Emission of atmospherically significant halocarbons by naturally occurring and farmed

598   tropical macroalgae, Biogeosciences, 10, 3615–3633, doi:10.5194/bg-10-3615-2013, 2013.

599

600   Liang, Q., Stolarski, R. S., Kawa, S. R., Nielsen, J. E., Douglass, A. R., Rodriguez, J. M.,

601   Blake, D. R., Atlas, E. L., and Ott, L. E.: Finding the missing stratospheric Bry: a global

602   modeling study of CHBr3 and CH2Br2, Atmos. Chem. Phys., 10, 2269–2286,

603   doi:10.5194/acp-10-2269-2010, 2010.

604

605   McKeen, S. A. and Liu, S. C.: Hydrocarbon ratios and photochemical history of air masses,

606   Geophys. Res. Lett., 20, 2363–2366, 1993.

607

608   Montzka, S.A., S. Reimann, A. Engel, K. Krüger, S. O'Doherty, W.T. Sturges, Ozone-

609   Depleting Substances (ODSs) and Related Chemicals, Chapter 4 in *Scientific Assessment of*

610   *Ozone Depletion: 2010, Global Ozone Research and Monitoring Project–Report No. 52*, 516

611   pp., World Meteorological Organization, 2011.

612

613 Moore, R.M., Webb, M., Tokarczyk, R. And Wever, R. Bromoperoxidase and

614 iodoperoxidase enzumes and production of halogenated methanes in marine diatom cultures.

615 Journal of Geophysical Research C: Oceans vol. 101(C9) pp.20899-20908, 1996.

616

617 O'Brien, L. M., Harris, N. R. P., Robinson, A. D., Gostlow, B., Warwick, N., Yang, X., and

618 Pyle, J. A.,Bromocarbons in the tropical marine boundary layer at the Cape Verde

619 Observatory measurements and modelling, Atmos. Chem. Phys., 9, 9083–9099,

620 doi:10.5194/acp-9-9083-9099, 2009.

621

622 Ordóñez C., Lamarque, J.-F., Tilmes, S., Kinnison, D. E., Atlas, E. L., Blake, D. R., Sousa

623 Santos, G., Brasseur, G., and Saiz-Lopez, A.: Bromine and iodine chemistry in a global

624 chemistry-climate model: description and evaluation of very short-lived oceanic sources,

625 Atmos. Chem. Phys., 12, 1423–1447, doi:10.5194/acp-12-1423-2012, 2012.

626

627 Pyle, J. A., Ashfold, M. J, Harris, N. R. P., Robinson, A. D., Warwick, N. J., Carver, G. D.,

628 Gostlow, B., O'Brien, L. M., Manning, A. J., Phang, S. M., Yong, S. E., Leong, K. P., Ung,

629 H. E., and Ong, S., Bromoform in the tropical boundary layer of the Marintime Continent

630 during OP3. Atmos. Chem. Phys., 11: 529-542, 2011.

631

632 Quack, B. and Suess, E.: Volatile halogenated hydrocarbons over the western Pacific 43° and

633 4° N, J. Geophys. Res., 104, 1663– 1678, 1999.

634

635 Quack, B., Atlas, E., Petrick, G., Stroud, V., Schauffler, S., and Wallace, D. W. R.: Oceanic

636 bromoform sources for the tropical atmosphere, Geophys. Res. Lett., 31, L23S05,

637 doi:10.1029/2004GL020597, 2004.

638

639 Salawitch, R. J, Atmospheric chemistry: Biogenic bromine, Nature, 439, 275–277,

640 doi:10.1038/439275a, 2006.

641

642 Sala, S., Bönisch, H., Keber, T., Oram, D. E., Mills, G., and Engel, A.: Deriving an

643 atmospheric budget of total organic bromine using airborne in-situ measurements from the

644 Western Pacific during SHIVA, Atmos. Chem. Phys. Discuss., 14, 4957-5012,

645 doi:10.5194/acpd-14-4957-2014, 2014.

646

647 Seh-Lin Keng, F., Phang, S. M., Abd Rahman, N., Leedham, E., Hughes, C., Pyle, J. A.,

648 Harris, N. R. P., Robinson, A., and Sturges, W. T.: Volatile halocarbon emissions by three

649 tropical brown seaweeds under different irradiances, J. Appl. Phycol., 25, 1377–1386,

650 doi:10.1007/s10811-013-9990-x, 2013.

651

652 Sturges, W. T., Sullivan, C. W., Schnell, R. C., Heidt, L. E., and Pollack, W. H.:

653 Bromoalkane production by Antartic ice algae. Tellus B 45, 120-126. 1993.

654

655 Tan, C. K., Ishizaka, J., Matsumura, S., Yusoff, F. M., and Mohamed, M. I. H.: Seasonal

656 variability of SeaWiFS chlorophyll a in the Malacca Strait in relation to Asian monsoon.

657 Continental Shelf Res., 26: 168-178, 2006.

658 Warwick, N. J., Pyle, J. A., Carver, G. D., Yang, X., Savage, N. H., O'Connor, F. M., and

659 Cox, R. A.: Global modelling of biogenic bromocarbons, J. Geophys. Res., 111, D24305,

660 doi:10.1029/2006JD007264, 2006.

661

662 World Meteorological Organization (WMO)/United Nations Environment Programme

663 (UNEP): Scientific Assessment of Ozone Depletion: 2006, World Meteorological

664 Organization, Global Ozone Research and Monitoring Project, Report No. 50, Geneva,

665 Switzerland, 2007.

666

667 Worton, D. R., Mills, G. P., Oram, D. E., and Sturges, W. T.: Gas chromatography negative

668 ion chemical ionization mass spectrometry: application to the detection of alkyl nitrates and

669 halocarbons in the atmosphere, J. Chromatogr. A, 1201, 112–119, 2008.

670

671 Yang, Y., Abraham, N. L., Archibald, A. T., Braesicke, P., Keeble, J., Telford, P., Warwick,

672 N. J and Pyle, J. A: How sensitive is the recovery of stratospheric ozone to changes in

673 concentrations of very short lived bromocarbons? Atmos. Chem. Phys. Discuss., 14, 1919–

674 1969, submitted, 2014.

675

676 Yokouchi, Y., Mukai, H., Yamamoto, H., Otsuki, A., Saitoh, C., and Nojiri, Y., Distribution

677 of methyl iodide, ethyl iodide, bromoform, and dibromomethane over the ocean (east and

678 southeast Asian seas and western Pacific). J. Geophys Res, 102, 8805-8809, 1997.

679

680   Yokouchi, Y., Hasebe, F., Fujiwar, M., Takashima, H., Shiotani, M., Nishi, N., Kanaya Y.,

681   Hashimoto, S., Fraser, ,P., Toom-Sauntry, D. Mukai, H., and Nojiri, Y. Correlations and

682   emission ratios among bromoform, dibromochloromethane, and dibromomethane in the

683   atmosphere. J. Geophys Res, 110, D23309, doi:10.1029/2005JD006303, 2005.
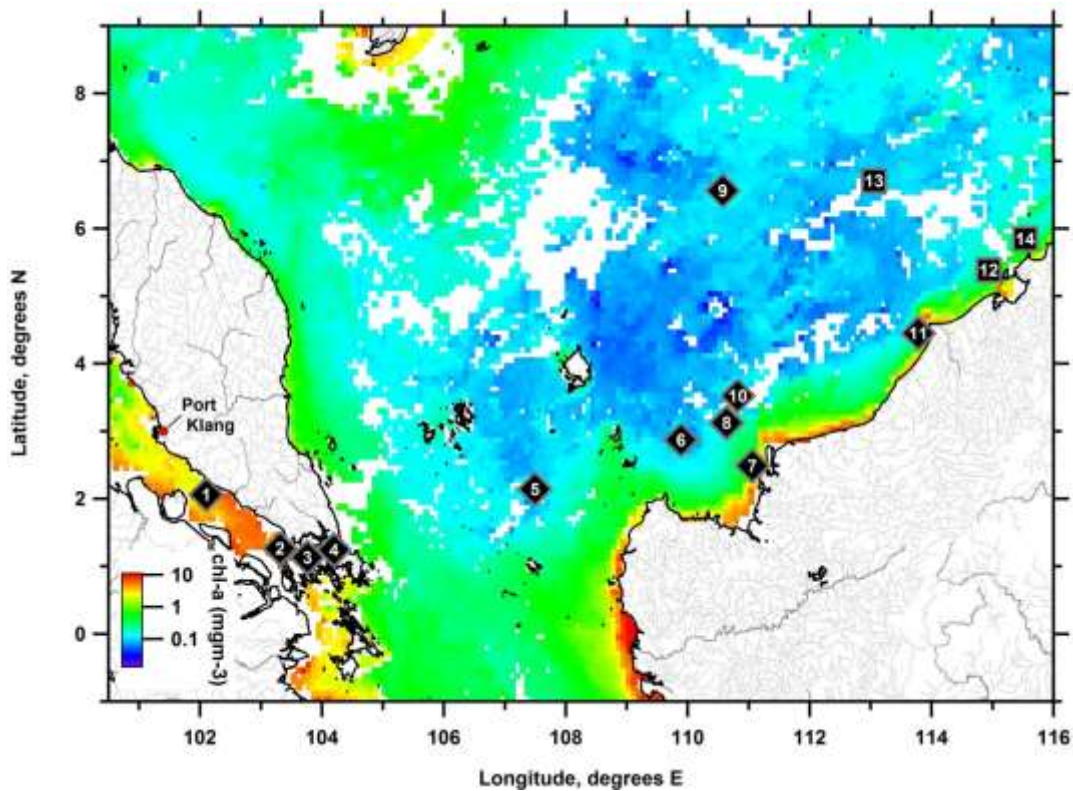
684
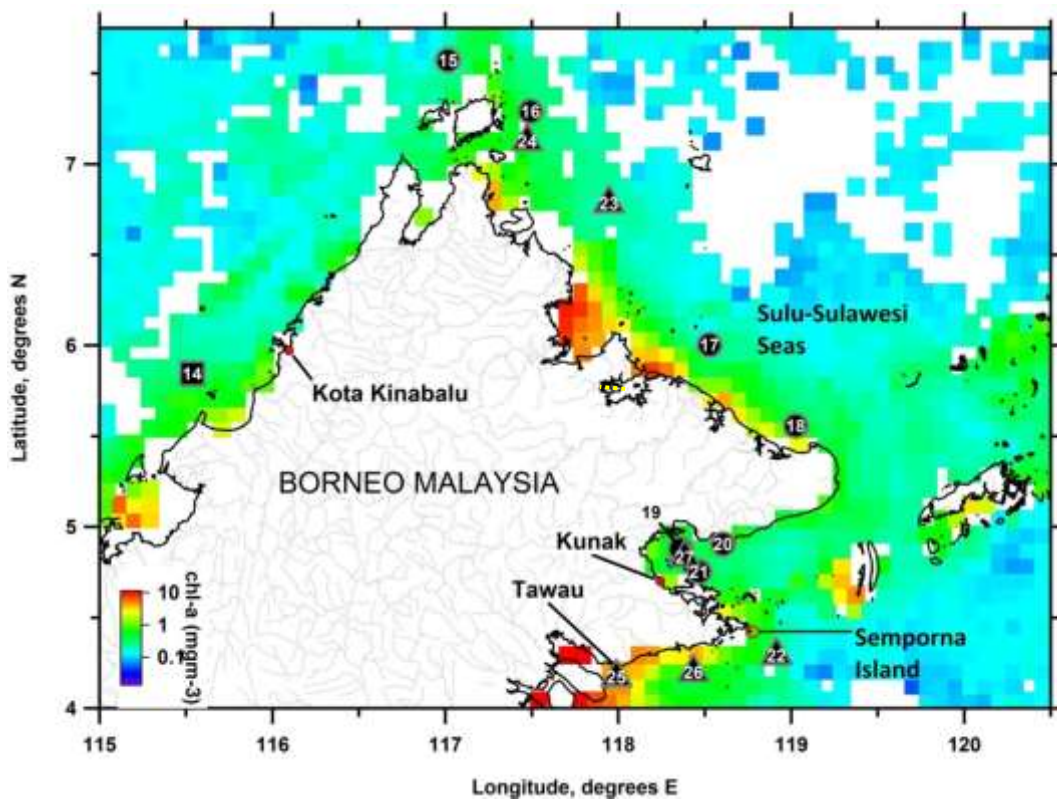
685

686

687

688

689

690

691
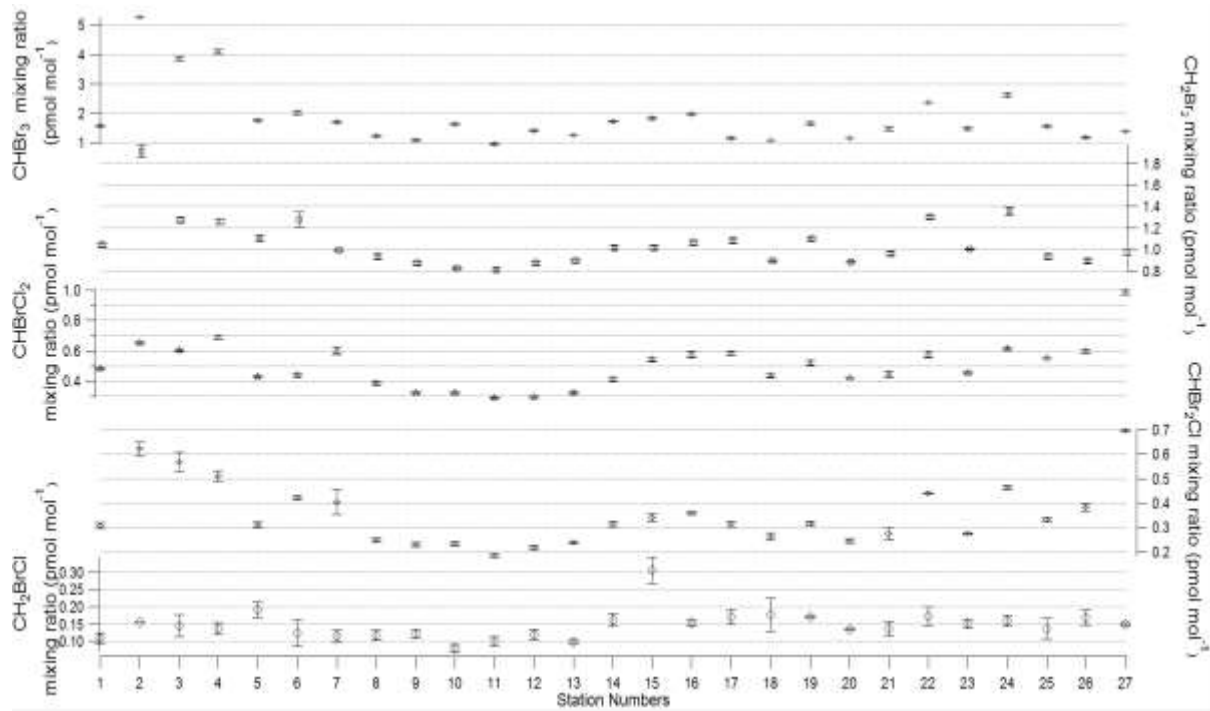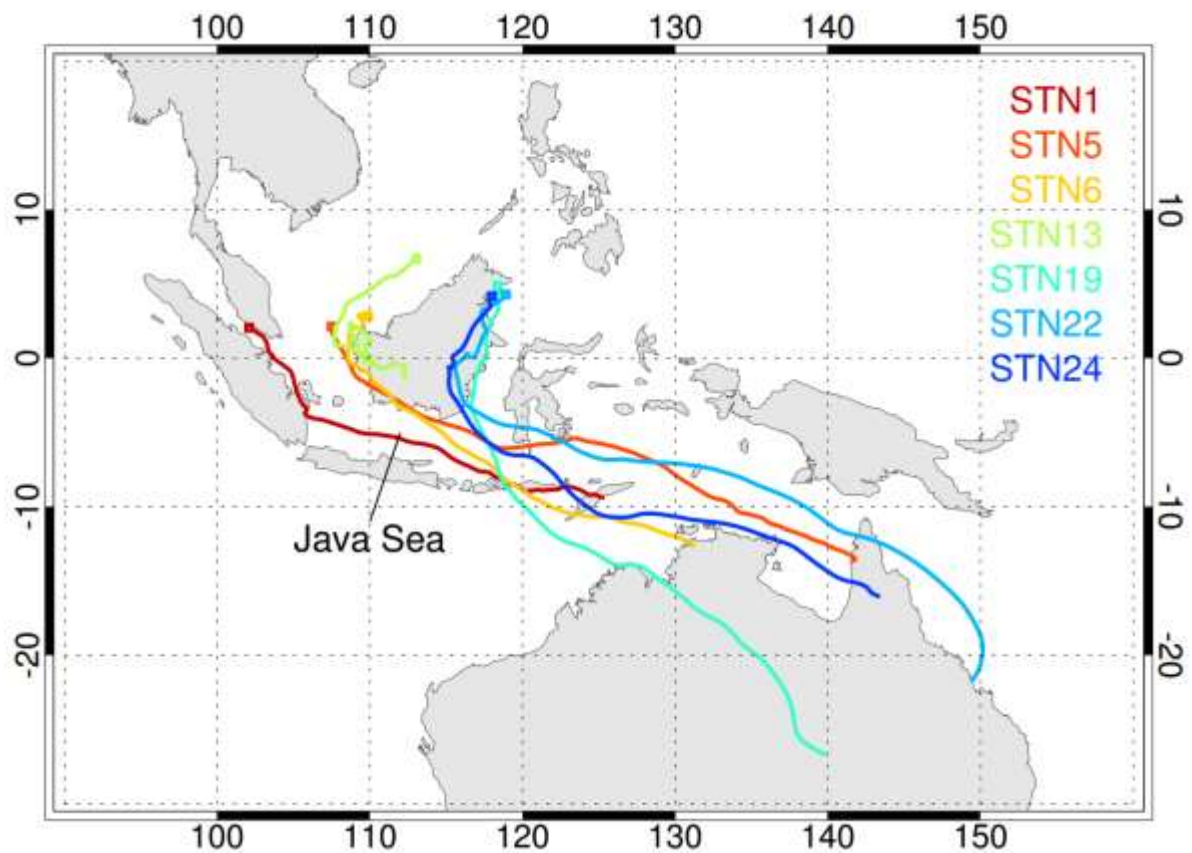
692

693

694

695

696

697

698

699 **List of figures**

700

701

702 **Figure 1:** Sampling locations overlaid with SeaWiFS chl-a during PESC-09 (Labels:
703 diamond = 1st leg; square = 2nd leg; circle = 3rd leg and triangle = 4th leg).

**Figure 2:** Bromocarbon mixing ratios for each station during PESC-09.

Figure 3: 10 days air distribution backward trajectories calculated from the NOAA HYSPLIT model for selected stations.

710
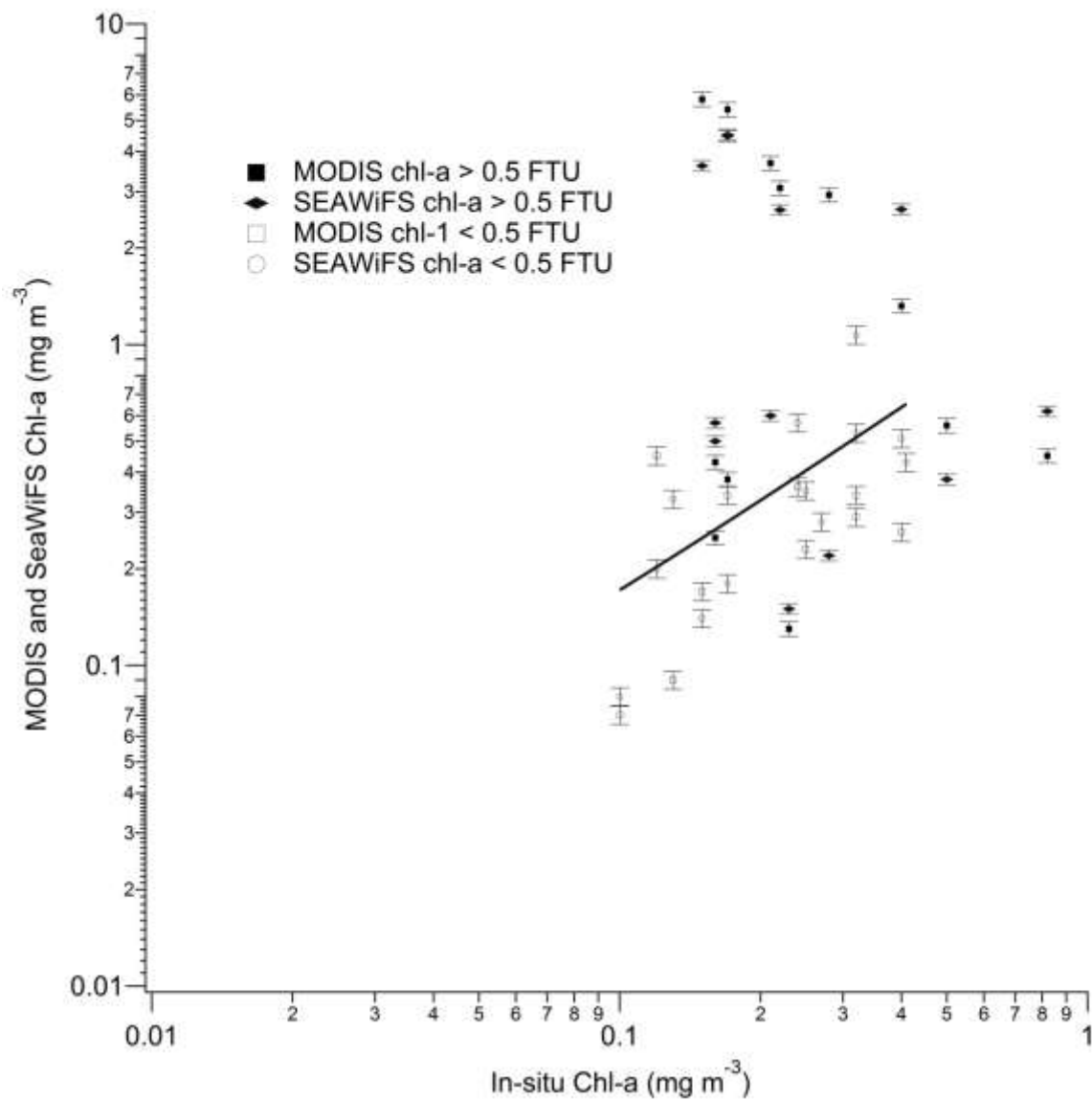
Figure 4: Chl-*a* concentration from the satellite data plotted against *in-situ* chl-*a*. The solid
symbols represent samples where turbidity was >0.5 FTU, and open symbols for turbidities
<0.5 FTU. The line is a linear fit to the lower turbidity samples.
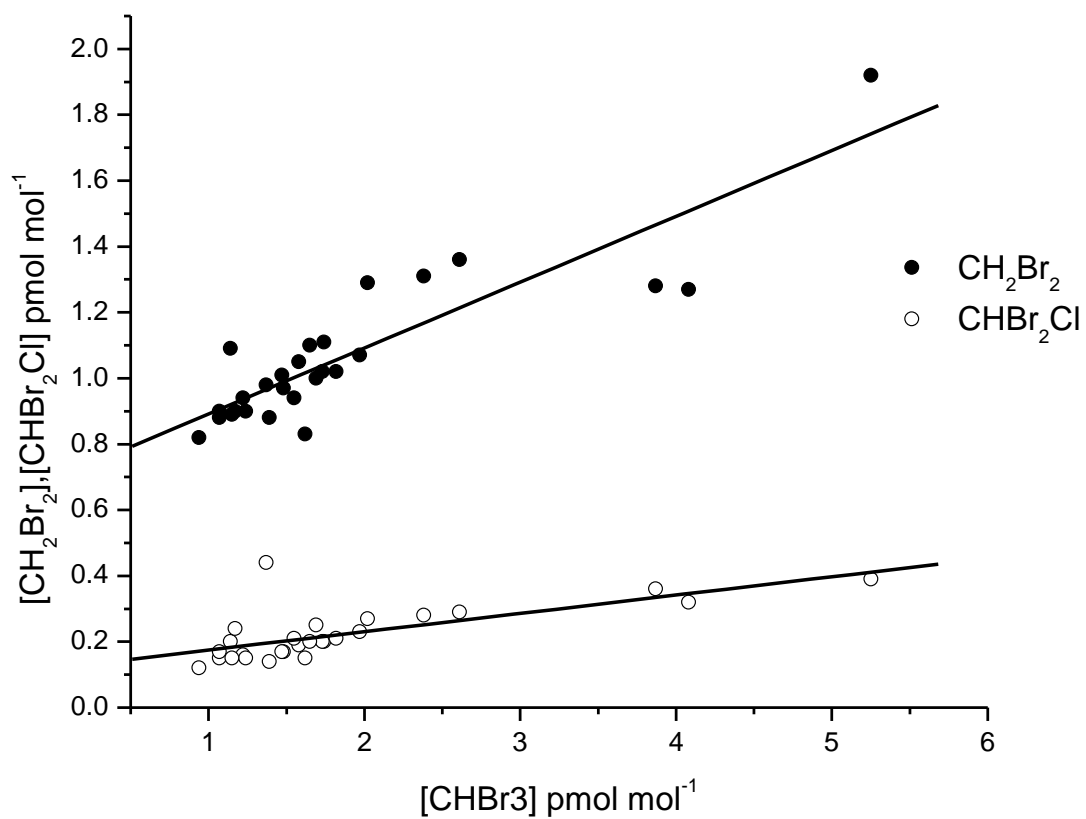
a)

b)

c)

d)
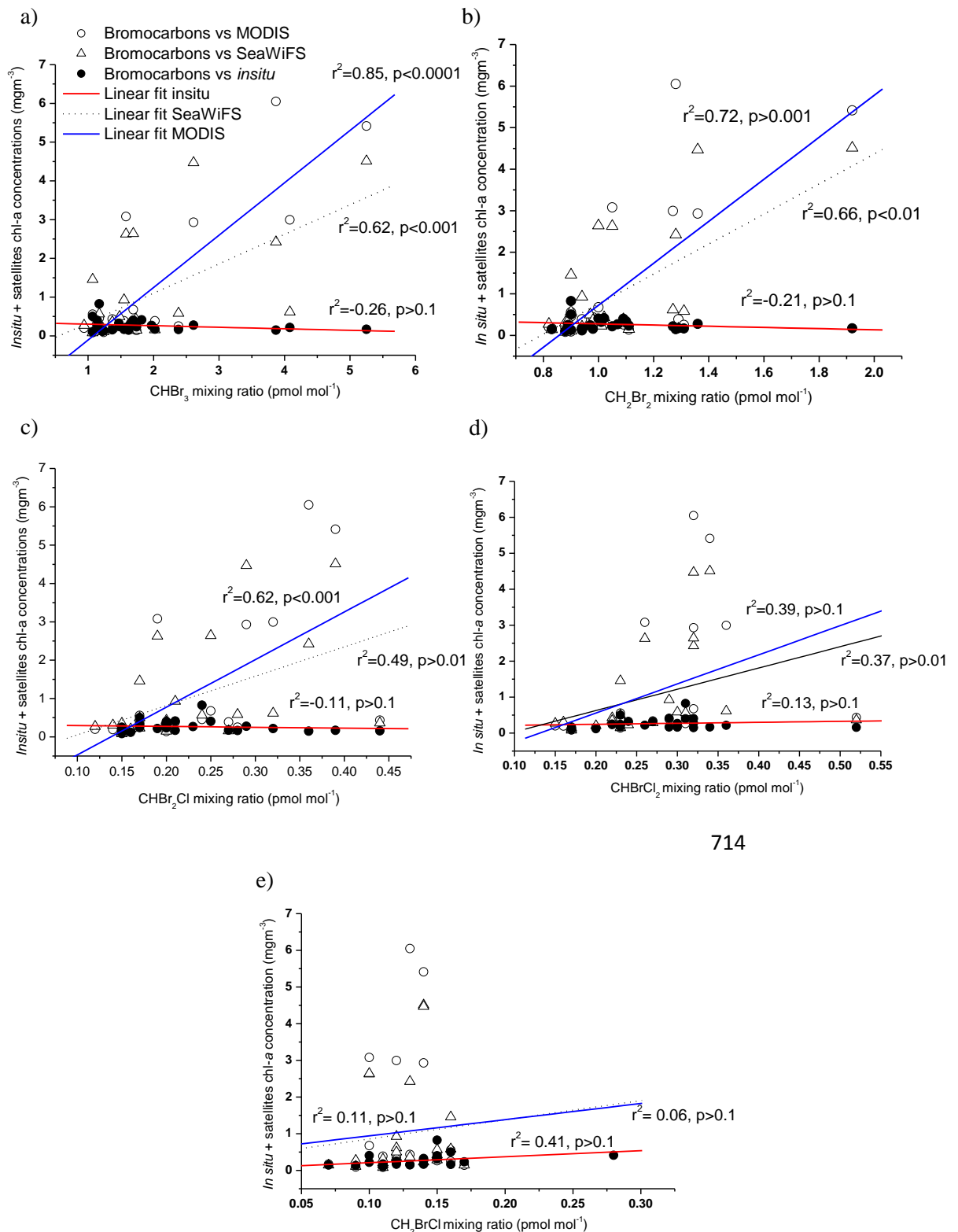
714

715

716

717

718

719

720

721

722

Figure 5: Monthly June-July 2009 *in situ* and satellite chl-*a* concentration as a function of VSLS bromocarbons mixing ratios a) $CHBr_3$, b) CH_2Br_2 c) $CHBr_2Cl$ d) $CHBrCl_2$ and e) CH_2BrCl.

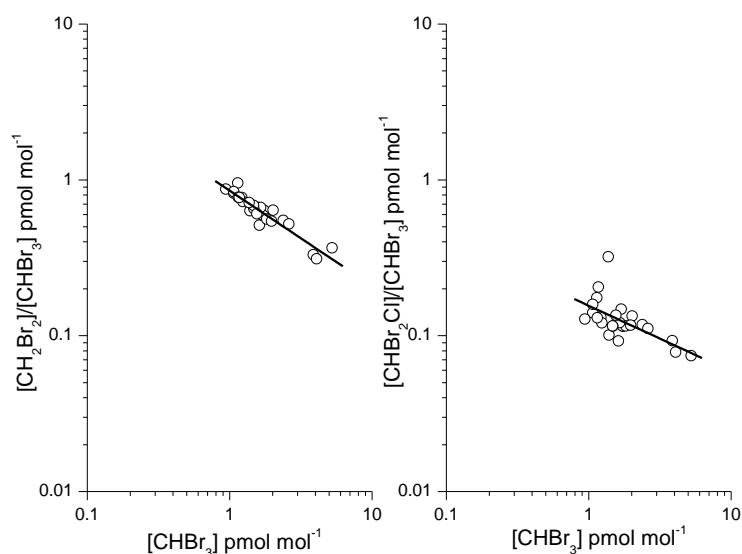**Figure 6:** Plot for correlations of CH_2Br_2 and $CHBr_2Cl$ versus $CHBr_3$ concentrations.
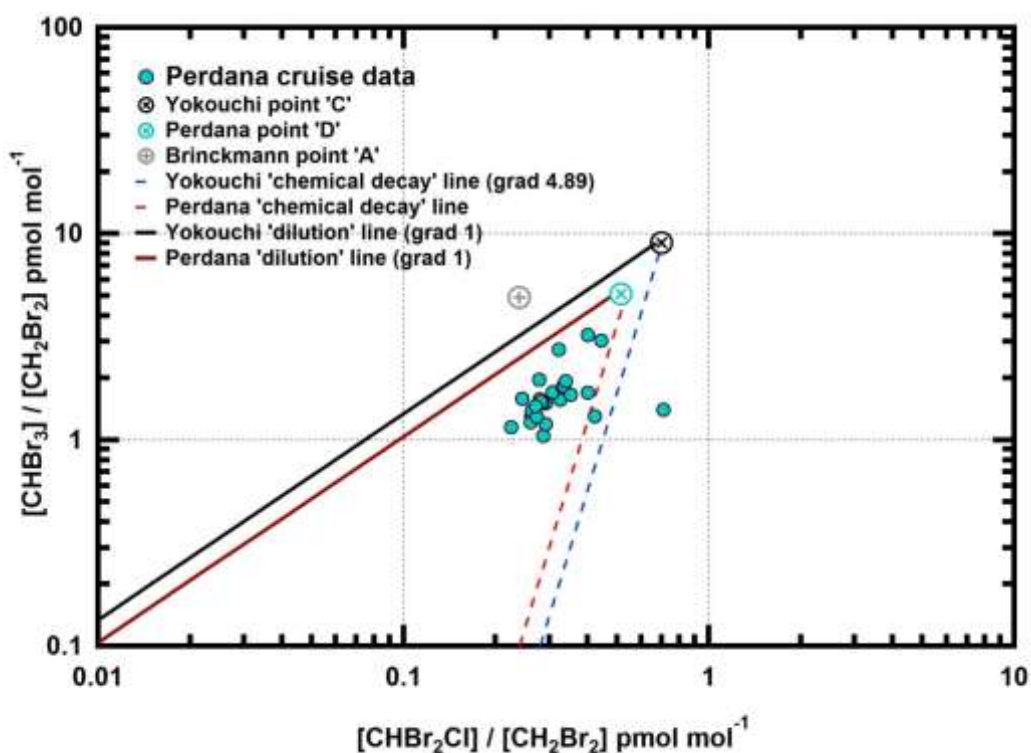
a)

733

734   b)

735

Figure 7: a) Log-log plot CH$_2$Br$_2$/CHBr$_3$ and CHBr$_2$Cl/CHBr$_3$ against CHBr$_3$ and 7b)
Log-log plots of CHBr$_3$/CH$_2$Br$_2$ against CHBr$_2$Cl/CH$_2$Br$_2$ for all stations during Perdana
Cruise, following Yokouchi et al. (2005) and Brinckmann et al., (2011). The solid line is the
dilution line 1:1 and the solid dash line is the chemical decay line which estimated from the
lifetime of the 3 species in the atmosphere. In this case, we have followed the example of
Yokouchi et al. (2005) by using the lifetimes of 26 days (CHBr$_3$), 69 days (CHBr$_2$Cl) and 120
days (CH$_2$Br$_2$). Thus the decay line has a slope of 4.89. The black point at the top of the data

743 set is the point C in Yokouchi et al. (2005) and grey point is the point A in Brinckmann et al.,
744 (2011) log-log plots where $CHBr_3/CH_2Br_2$ to be around 9 and $CHBr_2Cl/CH_2Br_2$ to be around
745 0.7 from Yokouchi et al. (2005) and around 5 for $CHBr_3/CH_2Br_2$ and 0.2 for
746 $CHBr_2Cl/CH_2Br_2$ from Brinckmann et al. (2011).

747

748

749

750

751

752

753

754

755

756

757

758

759

760

761

762

763

764

765

766 **Table 1:** Mean, standard deviation (in brackets) and range (in italics) values of the measured halocarbon concentrations in this work and values
767 from the literature based on tropical ocean areas (n.m. not mentioned).

Area	Author	No. of samples	CHBr$_3$ Mean (std) *range*	CHBr$_2$Cl Mean (std) *range*	CH$_2$Br$_2$ Mean (std) *range*	CHBrCl$_2$ Mean (std) *range*	CH$_2$BrCl Mean (std) *range*	*Chl-a* (mgm^{-3}) (std)	Turbidity (FTU)
Bromocarbon's Mixing ratios									
Strait of Malacca									
coastal	This study	4	3.69 (1.54) *1.85-5.25*	0.32(0.09) *0.19-0.39*	1.38(0.37) *1.05-1.92*	0.12 (0.02) *0.19-0.39*	0.12 (0.04) *0.1-0.14*	0.19(0.3)	3.33(1.22)
South China Sea									
Open ocean	This study	6	1.51 (0.4) *1.07-2.02*	0.21(0.05) 0.15-027	1.01(0.19) 0.88-1.29	0.22 (0.07) 0.17-0.32	0.10 (0.01) 0.09-0.11	0.17 (0.09)	0.19 (0.07)
coastal	This study	5	0.90(0.32) *0.82-1.02*	0.15(0.08) *0.12-0.2*	0.90(0.09) *0.82-1.02*	0.18(0.03) *0.15-0.22*	0.10 (0.03) *0.07-0.15*	0.22(0.12)	0.15(0.07)
Sulu-Sulawesi seas									
coastal	This study	12	1.60(0.5) *1.07-2.61*	0.23(0.08) *0.15-0.44*	1.04(0.16) *0.89-1.36*	0.3(0.08) *0.22-0.52*	0.15(0.04) *0.12-0.28*	0.32(0.2)	1.54(0.92)
Previous studies in tropical regions									
South east Asia 100-105°E	Youkouchi et al., 1995		1.2 (n.m) *0.3-7.1*		0.77(n.m) *0.38-1.42*				
Western Pacific 43°N, 150°E & 4°N, 113°E	Quack & Suess., 1999		1.2(n.m) *0.38-10.67*	0.2(n.m) *0.07-1.34*		0.28(n.m) *0.08-2.96*			
San Cristobal Island (Loberia)	Yokouchi et al., 2005		14.2 (10.1) *4.2-43.6*	1.5(1.0) *0.5-4.1*	3.2(1.5) *1.8-7.6*				
Christmas Island (Topono)	Yokouchi et al., 2005		23.8 (10.7) *16.3-31.4*	2.0 (0.7) *1.5-2.4*	3.0 (1.0) *2.3-3.7*				
Java Island	Yokouchi et al., 2005		0.9 (0.4) *0.4-1.6*	0.2 (0.2) *0.1-0.6*	0.9 (0.2) *0.6-1.5*				
Pacific Equator	Yokouchi et al., 2005		1.9(0.9) *0.8-3.5*	0.3(0.1) *0.1-0.6*	1.3(0.5) *0.2-1.9*				

768